

Structural and spectroscopic comparisons of tris(2-(diphenylphosphino)ethyl)aminecopper(I) tetrphenylborate, $[(NP_3)Cu](BPh_4)$, with gold(I) and silver(I) $[(NP_3)M]X$ ($X = BPh_4, NO_3, PF_6$) complexes

John P. Fackler, Jr.^{1,*}, Jennifer M. Forward, Tiffany Grant, Richard J. Staples

Department of Chemistry and Laboratory of Molecular Structure and Bonding, Texas A & M University, College Station, TX 77842-3012, USA

Received 25 November 1997; accepted 6 January 1998

Abstract

The ligand tris(2-(diphenylphosphino)ethyl)amine (NP_3) reacts with $CuCl$ in CH_2Cl_2 to produce the monomeric complex $[(NP_3)Cu](BPh_4)$, (**1**). Unlike the Au(I) and Ag(I) derivatives, this material is weakly 4-coordinate with a trigonal CuP_3 coordination and somewhat long Cu–N bonding to the tertiary N atom. Compound **1** crystallizes in the monoclinic space group $P2_1/n$ (No. 14) with cell constants: $a = 21.068(8) \text{ \AA}$, $b = 18.546(2) \text{ \AA}$, $c = 31.523(6) \text{ \AA}$, $\beta = 107.02(2)^\circ$ and $Z = 8$. Refinement of 12572 reflections and 1075 parameters yields $R = 0.0927$ and $R_w = 0.1980$. This structure completes the Cu, Ag, Au triad of NP_3 complexes. The 3-coordinate mononuclear and binuclear Au(I) NP_3 complexes, $[(NP_3)Au]X$ ($X = BPh_4, PF_6, NO_3$) and $[(NP_3)_2Au_2]X_2$ ($X = BPh_4, PF_6$), all show a brilliant luminescence under UV radiation. This emission has been studied in detail and is attributed to a metal-centered $p_z \rightarrow (d_{x^2-y^2}, d_{xy})$ transition. The Cu(I) complex is not luminescent in the visible spectral region. © 1998 Elsevier Science B.V. All rights reserved.

Keywords: tris(2-(diphenylphosphino)ethyl)amine; monomeric complex; luminescence

1. Introduction

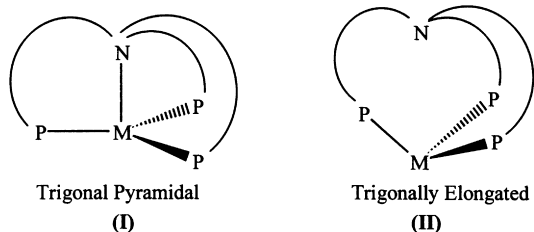
The potentially tetra dentate ligand tris(2-(diphenylphosphino)ethyl)amine (NP_3), which can coordinate to metal atoms using all four of its Group 15 atoms, has been shown to coordinate to a range of transition metal ions [1]. In mononuclear complexes the ligand generally wraps around the metal in an

umbrella-like fashion. However, two arrangements are found. The most common arrangement is a trigonal pyramidal geometry with one axial M–N and three equatorial M–P bonds, **I**. For many of the d^8 metal complexes found with this geometry, an additional axial ligand is coordinated to the metal center to satisfy the 16–18 electron rule, for example, $[(NP_3)Co(CS)]^+$ [2], $[(NP_3)Ni(Cl)]^+$ [3], and $[(NP_3)Pd(CH_3)]^+$ [4]. In some complexes [5], the M–N distance can be elongated with the metal moving out of the plane of the three phosphorus atoms, away from the nitrogen, giving a trigonally elongated geometry, **II**. The arrangement adopted depends on

* Corresponding author. Tel: 001 409 845 2835; Fax: 001 409 845 2373; e-mail: fackler@chemvx.tamu.edu

¹ Dedicated to a friend and colleague, Abraham Clearfield, on the occasion of his 70th birthday.

the electronic properties of the metal and the nature of the axial ligand.



Several complexes containing d^{10} metals and the NP_3 ligand have been structurally characterized and examples of both the trigonal pyramidal geometry and a trigonally elongated geometry have been observed. The $(\text{NP}_3)\text{Ni}(0)$ complex adopts the trigonal pyramidal geometry where there is no coligand coordinated to the nickel center [6,7]. The N-Ni-P angles are very close to 90° with the nickel atom situated in the plane of the three phosphorus atoms. The Ni-N distance is $2.178(7) \text{ \AA}$ which is relatively long but is within the usually observed Ni-N distances ($2.06\text{--}2.18 \text{ \AA}$) and is indicative of weak M-N bonding. The pyramidal coordination of the nitrogen, with its apex directed toward the Ni atom, suggests that the nitrogen electron lone pair can interact with the d_z^2 and p_z orbitals of the metal. It is the mixing of the p_z orbital with the d_z^2 orbital that produces a rehybridized orbital, with the two electrons in it, which is in the trans axial position. As the difference in energy between the d-orbital and empty p-atomic orbitals increases, for example on going from nickel to palladium, the extent of this d-p mixing decreases. This has the effect of increasing the repulsion between the NP_3 nitrogen atom and the metal center elongating the M-N bond. Such is the case for the palladium analog, $(\text{NP}_3)\text{Pd}(0)$, which has no co-ligand in the axial position [5]. The Pd-N bond is $2.69(2) \text{ \AA}$ and the structure of the complex shows the trigonally elongated geometry with the palladium lying out of the plane of the phosphorus atoms by 0.42 \AA away from the nitrogen center.

For the Cu, Ag, Au triad, the X-ray structures for the Ag(I) and Au(I) $d^{10} \text{NP}_3 [(\text{NP}_3)\text{M}]\text{X}$ ($\text{M} = \text{Au, Ag}$; $\text{X} = \text{PF}_6, \text{NO}_3, \text{BPh}_4$) complexes have been described [8]. Each of these complexes show a trigonally elongated geometry where the coordination of the metal center is approximately trigonal planar and there is no

strong interaction between the metal and the ligand nitrogen atom. However, the $[(\text{NP}_3)\text{AgONO}_2]$ complex shows a significantly longer $\text{Ag}\cdots\text{N}$ coordination, $2.924(4) \text{ \AA}$, than found in the $[(\text{NP}_3)\text{Ag}]\text{PF}_6$ complex, $2.662(3) \text{ \AA}$. The axial coordination of the nitrate, although weak, $\text{Ag}\cdots\text{O}$, $2.55(1) \text{ \AA}$, presumably is the cause for this difference in the $\text{Ag}\cdots\text{N}$ coordination. Also it is to be noted that the Ag-P distances are significantly longer, $2.477(3)\text{--}2.524(3) \text{ \AA}$, than the Au-P distances, $2.361(2)\text{--}2.369(2) \text{ \AA}$, for the isomorphous $[(\text{NP}_3)\text{Au}]\text{NO}_3$ complex. This observation of shorter M-P distances for Au(I) compared with Ag(I) is consistent with the smaller covalent radius of Au(I) compared with Ag(I) [9]. The gold(I) complexes of the NP_3 ligand show a luminescence in the solid state at room temperature. Several examples of three-coordinate, gold(I) complexes that show emission have been reported [10–12], including phosphine complexes soluble in water [13].

Since the emission [14] from three coordinate gold(I) and platinum(0) phosphine [15,16]² complexes is apparently associated with a transition which is orbitally and spin forbidden in trigonal coordinated d^{10} complexes (wherein the excitation energy is in the near UV), it seemed appropriate to ask if Cu(I) complexes of this NP_3 ligand would (i) have a trigonal planar CuP_3 coordination and (ii) also be luminescent. The energy separation between the 1S_0 and the 1D level in the Cu(I) ion is 26264 cm^{-1} , comparable with the 29620 cm^{-1} separation [17] in the gaseous Au(I) ion [18], and much smaller than the 46046 cm^{-1} separation for Ag(I). No luminescence is observed for the $[(\text{NP}_3)\text{Ag}]\text{X}$ complexes [9]. This paper reports the results of our observations on $[(\text{NP}_3)\text{Cu}]\text{PF}_6$.

2. Experimental

The reactions were carried out under an atmosphere of dry nitrogen using standard Schlenk line techniques. The complexes $[(\text{NP}_3)_2\text{Au}_2]\text{X}_2$ ($\text{X} = \text{BPh}_4$,

² Unfortunately the authors do not comment on luminescence as they describe the structure for the first homoleptic complex of Pt(0) formed with secondary phosphines which is rigorously trigonal in its PtP_3 geometry.

PF₆) and [(NP₃)Au]X (X = BPh₄, NO₃, PF₆) and [(NP₃)Ag](PF₆) were all synthesized using a previously published procedure [9]. The purity was checked by ³¹P{¹H} NMR and the unit cell dimensions were compared with previously reported data. The ligand, NP₃, was prepared according to the literature [19]. ³¹P{¹H} NMR spectra were recorded on a Varian XL-400 spectrometer. Emission and excitation spectra were measured on an SLM/AMINCO 8100 spectrofluorometer, using a Xe lamp. The data were corrected for instrumental response. Lifetime measurements were made using about 0.8 ns excitation pulses from the 355 nm third harmonic of a Quantal YG481 Nd–YAG laser.

MM2 calculations were performed using a CACHE molecular modeling system [20,21]. The initial structures were obtained from the crystal structure of the [(NP₃)Au]⁺ ion, followed by substitution of either Ag or Cu for the Au atom. The opposite configuration at the nitrogen center was minimized by initially substituting a hydrogen for the electron pair and then final minimization with the electron pair.

Synthesis of [(NP₃)Cu](BPh₄) (**1**). NP₃ (0.05 g, 7.66 × 10⁻⁵ mol) was added to a solution of Cu(I)Cl (0.0076 g, 7.66 × 10⁻⁵ mol) in CH₃CN/CH₂Cl₂ (5 mL/5 mL). The reaction was stirred for 30 min and then one equivalent of NaBPh₄ was added (0.026 g, 7.66 × 10⁻⁵ mol). After stirring the reaction for an additional 30 min the solvent was removed under reduced pressure to reveal a white solid. This solid was extracted with CH₂Cl₂ (3 × 5 mL) and then diethyl ether was added to precipitate a white crystalline solid (yield = 67%). Single crystals were grown from the layering of a CH₂Cl₂ solution of the product with benzene and hexane.

3. X-ray data collection and refinement of the structure

Crystallographic data were collected using an Enraf–Nonius FAST area detector system. Specific procedures used were adapted in part from those described by Scheidt and Turowska-Tyrk [22]. A colorless crystal of dimensions 0.4 × 0.4 × 0.5 mm was selected and mounted on a quartz fiber with silicone grease. The crystal was cooled to –60(2)°C using an Enraf–Nonius low temperature controller, model FR558-S.

Initial crystal evaluation and data collection was performed on an Enraf–Nonius FAST area detector system using the program MADNES [23] in conjunction with a 4-circle κ-axis goniometer equipped with graphite monochromated Mo radiation (λ_{Kα} = 0.71073 Å). The crystal was optically centered in the X-ray beam. Since the low temperature stream is co-linear with the phi axis when χ is 0, a χ angle of 45° was used in order to position the goniometer head out of the cold stream, thereby avoiding complications resulting from differential, time-dependent cooling of the goniometer head. Initial crystal evaluation typically consists of a 30 to 60° rotation about ω, with an exposure time of 30–60 s. The image obtained upon exposure was similar to that observed for a standard rotational photograph and revealed that the crystal was suitable for further investigation.

Reflections used for the unit cell determination were obtained by scanning images measured at intervals of 0.2° in a 10° range about ω. The exposure time was 10 s per image. Upon completion of the scans, ω was rotated 10° and another 10° scan was made at intervals of 0.2°. A total of six 10° regions were scanned in the range 0 < ω < 100°. To enhance spectral resolution, the crystal–detector distance had been moved to 60 cm and the detector swing angle (θ) was set to 0. A total of 250 reflections were obtained. Fifty of these reflections were used by the auto-indexing routine, ENDEX, found in the MADNES software, resulting in a preliminary primitive monoclinic unit cell. Refined cell dimensions (Table 1) were obtained by least-squares fitting of 250 reflections in the range 10 < 2θ < 24°. Cell dimensions and Laue symmetry were confirmed by axial images measured using a 30° rotation about ω, with an exposure time of 30 s. Data collection was performed by measuring a series of images at intervals of 0.3° about ω. The detector was set at a distance of 60 mm and a swing angle of 20°. Images were collected by scanning through four separate regions of space. One sweep of 110° about ω was made with κ = 33° (χ = 25°). Φ was then rotated 90° and a second 110° sweep was made. Finally, two 75° sweeps of ω were made with κ = –170° (χ = 98°); the second sweep was made with Φ rotated 90° from the first. This collection procedure allows for slightly more than a hemisphere of data to be collected. Based on the relative diffraction intensity, an exposure time of 20 s was selected. Exposure times may be varied

Table 1
Crystallographic data for $[(\text{NP}_3)\text{Cu}](\text{BPh}_4)$, (**1**)

$[(\text{NP}_3)\text{Cu}](\text{BPh}_4)$ (1)	
Chemical formula	$\text{C}_{67.5}\text{H}_{64}\text{BCl}_{2.5}\text{CuN}_3\text{P}$
Molecular weight	1145.1
Crystal size (mm)	$0.4 \times 0.4 \times 0.5$
Crystal system	Monoclinic
Space group	$\text{P}2_1/\text{n}$ (No. 14)
a (Å)	21.068(8)
b (Å)	18.546(2)
c (Å)	31.523(6)
β , deg	107.02(2)
V (Å ³)	11777(5)
Z	8
μ (mm ⁻¹)	0.608
D_c (g cm ⁻³)	1.292
Temp. (K)	298
Radiation (λ , Å)	Graphite-monochromated Mo $K\alpha$ (0.71073)
R , ^a R_w ^b	0.0927, 0.1980

$$^a R = \frac{\sum |F_o| - |F_c|}{\sum |F_o|}$$

$$^b R_w = \frac{\{\sum w(|F_o| - |F_c|)\}}{\sum w|F_o|}$$

between 3 and 40 s, depending on the intensity of the diffraction pattern. Throughout the data collection, the actual positions of reflections were compared with those predicted based on the orientation matrix. Reflections that occur outside the predicted 'shoebox' region were flagged. Raw data images that were obtained were immediately evaluated using an off-line version of MADNES. The method used for evaluation involved the use of a best fit ellipsoid that gives the lowest $\sigma(I)/I$ to determine the boundaries for strong reflections. The shapes and boundaries of weak reflections are then based on those of strong reflections in the same area of the detector [24–26]. The data were corrected for Lorentz and polarization effects by the MADNES program. Reflection profiles were fitted and values of F^2 and $\sigma(F^2)$ for each reflection were obtained by the program PROCOR, which uses a fitting algorithm developed by Kabsch [27,28]. Intensity data were examined for systematic absences by an in-house program that provides a concise listing of reflection classes to facilitate space group assignment. The reflection data file was also reformatted by the program for use with a SHELXL-93 structure refinement software package [29].

A total of 31350 data were obtained in the range $3.0 < 2\theta < 44.84^\circ$. Averaging of equivalent

reflections ($R_{\text{merge}} = 7.64\%$) yielded 12572 unique reflections of which 9565 were considered observed with $I > 2\sigma(I)$. No absorption correction was applied. The position of the metal atom was located using the direct methods program, SHELXS-86. The remaining non-hydrogen atoms were located in an alternating series of least-squares cycles and difference Fourier maps. One CH_2Cl_2 was found to be disordered near the inversion center. All non-hydrogen atoms were modelled anisotropically and the hydrogens placed in idealized positions for all atoms except for the disordered solvent. Final least squares refinement of 1075 parameters resulted in residuals R (based on F) and R_w (based on F^2 for all data)³ of 0.0927 and 0.24, respectively. The quality-of-fit was 1.15 based on F^2 for all data. A final difference Fourier revealed that the highest remaining peak of electron density was $0.98 \text{ e } \text{Å}^{-1}$ [3].

4. Structural results

The structure of $[(\text{NP}_3)\text{Cu}](\text{BPh}_4)$, **1**, is shown in Fig. 1. Details of the crystal structure determination are given in Table 1. The atomic coordinates for $[(\text{NP}_3)\text{Cu}](\text{BPh}_4)$ are given in Table 2 and selected bond distances and angles are given in Table 3. The complex crystallizes in the monoclinic space group $\text{P}2_1/\text{n}$ with two well-separated cations and two anions in the asymmetric unit. The bond distances and angles within each of the two related molecules are similar.

There is little to remark on the molecular structure of $[(\text{NP}_3)\text{Cu}](\text{BPh}_4)$, except to note that the apical N atom clearly coordinates to the copper(I). This does not happen with Au(I) and with Ag(I) the interaction is also very weak, with an Ag–N distance of 2.662 Å in the $[(\text{NP}_3)\text{Ag}]\text{PF}_6$, for example. The Cu–N distances in the Cu(I) complex are 2.275(7) Å and 2.301(7) Å for the two different molecules observed crystallographically. The coordination around the nitrogen center shows that the nitrogen lies closer to the copper than its neighboring carbon atoms.

³ R factors based on F^2 are statistically about twice as large as those based on F and an R -index based on all data is inevitably larger than one based only on data with F greater than a given threshold.

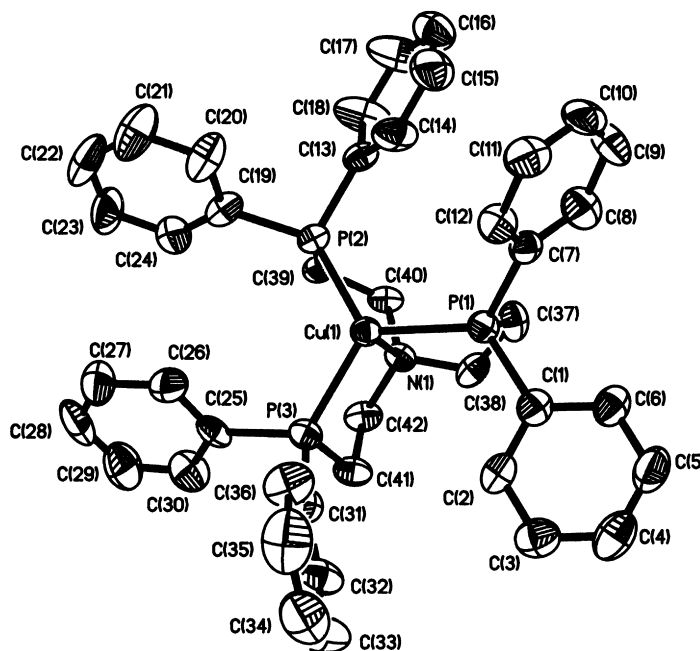


Fig. 1. Molecular structure of the cation $[(NP_3)Cu]^+$ of **1**.

The C–N–C bond angles are in the range 110.2° – 111.6° , indicating that the geometry of the nitrogen is approximately tetrahedral with the lone pair orbital facing towards the metal center.

The coordination of the copper center with the three phosphorus atoms is essentially trigonal planar with the P–Au–P angles in the range 116° – 122° .

The Cu–P bond lengths are all similar (2.24–2.27 Å) and approximately form an equilateral triangle around the gold(I) center. The copper atom lies slightly out of this plane by 0.144 Å and 0.159 Å for the two different molecules, in a direction away from the nitrogen. The observed Cu–P distances are about 0.2 Å shorter than those found with the Ag(I)

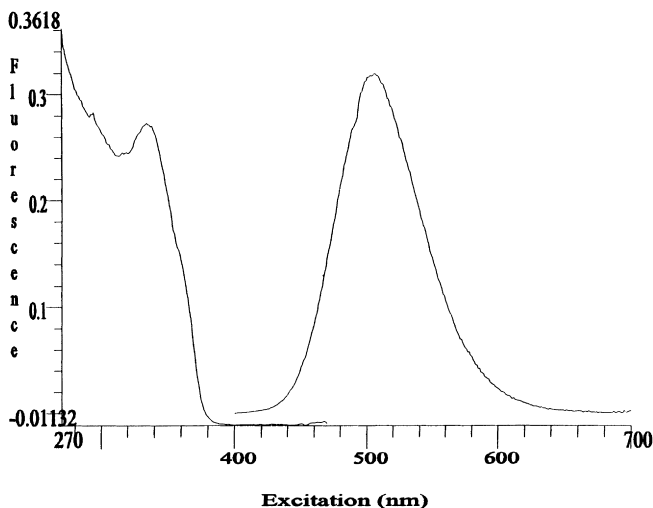


Fig. 2. Excitation and emission spectra for $[(NP_3)Au](PF_6)$.

Table 2

Atomic coordinates ($\times 10^4$) and equivalent isotropic displacement parameters ($\text{\AA}^2 \times 10^3$) for $[(\text{NP}_3)\text{Cu}](\text{BPh}_4)_2(\mathbf{1})$

	x	y	z	U(eq)
Cu(1)	6406(1)	6995(1)	1628(1)	31(1)
Cu(2)	1368(1)	7258(1)	1517(1)	35(1)
P(1)	5570(1)	7691(1)	1715(1)	34(1)
P(2)	6491(1)	5823(1)	1846(1)	34(1)
P(3)	7043(1)	7343(1)	1206(1)	35(1)
P(4)	1443(1)	6080(1)	1716(1)	36(1)
P(5)	2069(1)	7646(2)	1148(1)	39(1)
P(6)	479(1)	7908(1)	1553(1)	37(1)
N(1)	5671(3)	6594(4)	990(2)	32(2)
N(2)	711(3)	6879(4)	935(2)	39(2)
C(1)	5451(5)	8636(5)	1516(3)	42(3)
C(2)	5889(5)	8945(6)	1319(3)	46(3)
C(3)	5784(5)	9631(6)	1147(4)	56(3)
C(4)	5244(6)	10018(6)	1176(4)	62(3)
C(5)	4806(6)	9722(7)	1368(4)	65(3)
C(6)	4894(5)	9028(6)	1532(3)	49(3)
C(7)	5345(5)	7701(5)	2237(3)	38(2)
C(8)	4714(5)	7541(6)	2258(4)	56(3)
C(9)	4584(6)	7517(7)	2666(4)	66(3)
C(10)	5078(7)	7665(6)	3040(4)	63(3)
C(11)	5704(6)	7843(6)	3026(4)	57(3)
C(12)	5841(5)	7854(5)	2623(3)	44(3)
C(13)	5984(5)	5549(5)	2199(3)	36(2)
C(14)	5945(6)	6011(6)	2531(4)	59(3)
C(15)	5582(7)	5838(7)	2819(4)	74(4)
C(16)	5239(5)	5198(7)	2767(4)	62(3)
C(17)	5290(7)	4735(8)	2451(4)	86(5)
C(18)	5665(6)	4908(7)	2166(4)	73(4)
C(19)	7236(5)	5284(5)	2069(3)	43(3)
C(20)	7510(6)	5271(6)	2527(4)	64(3)
C(21)	8087(6)	4887(7)	2719(4)	77(4)
C(22)	8394(6)	4509(6)	2460(5)	75(4)
C(23)	8124(6)	4525(6)	2006(5)	72(4)
C(24)	7556(5)	4919(6)	1814(4)	60(3)
C(25)	7704(5)	6739(5)	1151(3)	38(2)
C(26)	8134(5)	6482(6)	1543(4)	55(3)
C(27)	8660(6)	6034(7)	1518(5)	71(4)
C(28)	8736(6)	5826(7)	1120(6)	71(4)
C(29)	8305(6)	6089(7)	738(5)	72(4)
C(30)	7793(6)	6539(7)	749(4)	60(3)
C(31)	7428(5)	8227(5)	1247(3)	44(3)
C(32)	7384(6)	8676(6)	901(4)	58(3)
C(33)	7679(8)	9351(7)	956(5)	82(4)
C(34)	8025(7)	9576(8)	1362(6)	79(4)
C(35)	8096(6)	9137(8)	1723(5)	84(4)
C(36)	7790(5)	8465(6)	1672(4)	60(3)
C(37)	4877(4)	7224(5)	1314(3)	44(3)
C(38)	5077(4)	7050(5)	903(3)	40(3)
C(39)	6114(5)	5406(5)	1308(3)	42(3)
C(40)	5500(4)	5827(5)	1051(3)	33(2)
C(41)	6402(5)	7332(5)	662(3)	41(2)
C(42)	5983(5)	6650(5)	626(3)	40(2)

Table 2 continued

	x	y	z	U(eq)
C(43)	876(4)	5696(5)	1997(3)	38(2)
C(44)	747(5)	6091(6)	2333(4)	57(3)
C(45)	355(6)	5817(8)	2576(4)	69(4)
C(46)	77(6)	5144(8)	2483(4)	67(4)
C(47)	195(6)	4761(8)	2149(5)	83(4)
C(48)	587(6)	5025(6)	1906(4)	67(3)
C(49)	2217(5)	5618(5)	1995(3)	41(3)
C(50)	2413(5)	4972(6)	1842(4)	57(3)
C(51)	2997(6)	4648(7)	2066(4)	70(4)
C(52)	3390(6)	4958(8)	2446(5)	82(4)
C(53)	3216(6)	5590(8)	2606(4)	79(4)
C(54)	2625(5)	5918(7)	2382(4)	66(3)
C(55)	2701(4)	7020(5)	1075(3)	40(2)
C(56)	3064(5)	6623(6)	1444(4)	54(3)
C(57)	3520(5)	6101(6)	1387(5)	62(3)
C(58)	3593(6)	5994(7)	974(5)	63(3)
C(59)	3263(6)	6389(7)	626(4)	61(3)
C(60)	2814(5)	6903(6)	666(4)	54(3)
C(61)	2486(5)	8524(5)	1257(4)	44(3)
C(62)	2694(6)	8773(7)	1681(4)	80(4)
C(63)	2989(7)	9439(8)	1791(5)	91(5)
C(64)	3076(7)	9862(8)	1461(7)	94(5)
C(65)	2883(8)	9620(10)	1039(7)	104(5)
C(66)	2581(7)	8955(8)	925(4)	79(4)
C(67)	355(5)	8846(5)	1373(3)	40(2)
C(68)	912(6)	9255(6)	1399(3)	54(3)
C(69)	838(7)	9989(7)	1280(4)	68(3)
C(70)	221(8)	10295(7)	1137(4)	67(4)
C(71)	-337(7)	9882(7)	1104(4)	69(4)
C(72)	-271(6)	9164(7)	1223(4)	58(3)
C(73)	195(5)	7882(5)	2047(3)	42(3)
C(74)	-435(5)	7698(6)	2040(4)	55(3)
C(75)	-598(6)	7634(8)	2431(5)	77(4)
C(76)	-139(6)	7744(7)	2833(4)	63(3)
C(77)	494(6)	7951(6)	2844(3)	54(3)
C(78)	661(5)	8016(5)	2459(3)	40(2)
C(79)	1187(5)	5703(6)	1159(3)	45(3)
C(80)	585(5)	6095(5)	871(3)	43(3)
C(81)	1477(5)	7697(6)	597(3)	47(3)
C(82)	1074(5)	7008(6)	500(3)	47(3)
C(83)	-161(4)	7415(6)	1129(3)	45(3)
C(84)	82(4)	7287(5)	728(3)	44(3)
B(1)	5789(5)	2980(6)	778(4)	40(3)
B(2)	1168(5)	3050(6)	779(4)	35(3)
C(101)	6145(4)	3677(5)	603(3)	34(2)
C(102)	5780(5)	4204(5)	320(3)	39(2)
C(103)	6060(5)	4769(6)	147(3)	46(3)
C(104)	6734(5)	4836(6)	269(3)	49(3)
C(105)	7124(5)	4339(6)	540(3)	53(3)
C(106)	6832(5)	3764(5)	707(3)	42(2)
C(107)	5698(4)	2328(5)	407(3)	38(2)
C(108)	5263(5)	1751(6)	384(4)	58(3)
C(109)	5205(6)	1175(7)	88(4)	67(3)

Table 2 continued

	x	y	z	U(eq)
C(110)	5588(6)	1163(7)	-188(4)	69(3)
C(111)	6016(5)	1711(6)	-191(4)	55(3)
C(112)	6068(5)	2293(5)	107(3)	42(2)
C(113)	6237(4)	2705(5)	1265(3)	37(2)
C(114)	6637(5)	3157(6)	1590(3)	47(3)
C(115)	7008(5)	2918(6)	2006(4)	53(3)
C(116)	6988(5)	2225(6)	2116(4)	59(3)
C(117)	6591(6)	1757(7)	1831(4)	67(3)
C(118)	6225(5)	1986(6)	1404(3)	51(3)
C(119)	5061(4)	3269(5)	823(3)	35(2)
C(120)	5045(5)	3716(5)	1174(3)	42(2)
C(121)	4467(5)	4030(6)	1210(4)	56(3)
C(122)	3873(5)	3898(6)	893(3)	53(3)
C(123)	3862(5)	3449(6)	549(4)	52(3)
C(124)	4440(4)	3137(5)	514(3)	44(3)
C(125)	1360(4)	2384(5)	497(3)	38(2)
C(126)	1407(5)	1664(6)	664(4)	52(3)
C(127)	1569(5)	1088(7)	434(4)	63(3)
C(128)	1660(6)	1187(7)	31(4)	68(3)
C(129)	1636(5)	1869(6)	-143(4)	61(3)
C(130)	1480(5)	2460(6)	88(3)	45(3)
C(131)	1326(4)	3836(5)	561(3)	31(2)
C(132)	845(4)	4205(5)	228(3)	37(2)
C(133)	976(4)	4830(5)	35(3)	36(2)
C(134)	1609(4)	5116(5)	159(3)	41(2)
C(135)	2094(5)	4769(6)	483(3)	46(3)
C(136)	1951(4)	4136(5)	677(3)	39(2)
C(137)	368(4)	3017(5)	751(3)	34(2)
C(138)	-11(4)	2395(5)	657(3)	40(2)
C(140)	-980(5)	2965(6)	744(3)	55(3)
C(141)	-629(5)	3599(6)	838(3)	51(3)
C(142)	39(4)	3616(5)	851(3)	41(2)
C(143)	1627(4)	2994(5)	1298(3)	36(2)
C(144)	1427(5)	3252(5)	1649(3)	43(3)
C(145)	1817(5)	3208(6)	2092(4)	55(3)
C(146)	2420(5)	2871(6)	2185(4)	53(3)
C(147)	2654(5)	2621(6)	1858(3)	54(3)
C(148)	2255(5)	2687(6)	1414(3)	50(3)
C(139)	-674(5)	2369(6)	653(3)	50(3)
Cl(4)	7270(2)	6168(2)	4595(1)	106(1)
Cl(3)	3869(2)	11646(2)	1227(1)	97(1)
Cl(2)	3541(2)	11029(2)	354(1)	103(1)
Cl(1)	7001(2)	6683(3)	3700(2)	112(1)
C(202)	3317(6)	11651(8)	706(4)	84(4)
C(201)	7601(7)	6470(10)	4181(5)	103(5)
Cl(5)	-749(4)	10600(4)	-33(3)	92
Cl(5B)	190	9491	65	130
C(203)	52	10560	-54(3)	50

U(eq) is defined as 1/3 the trace of the orthogonized U_{ij} tensor.

NP_3 complexes, and about 0.1 Å shorter than those found in the Au(I) complexes.

MM2 calculations performed on the CAChe molecular modeling system showed that the nitrogen lone pair of electrons bonding to the Cu(I) is energetically more favorable by more than 100 kcal mol⁻¹ when directed towards the P_3 plane, than when the lone pair is directed away from the P_3 plane. These calculations also place the metal atom out of the P_3 plane away from the nitrogen atom.

5. Spectroscopic results

These luminescence spectra have been investigated in more detail and the emissions obtained are summarized in Table 4, where it can be seen that only the Au(I) derivatives emit in the visible region. Fig. 2 shows the excitation and emission spectra measured for $[(\text{NP}_3)\text{Au}](\text{PF}_6)$ in the solid state at 298 K. The lifetimes for the Au(I) NP_3 complexes vary from 1–9 μs. The reason for the observation of two different components to the lifetimes is not fully understood but it may be related to the presence of the low energy π and π^* orbitals associated with the phenyl rings of the NP_3 ligand. The 3-coordinate Au(I) phosphine complex studied by McCleskey and Gray [10] and McCleskey et al. [30] $[(\text{dcpe})_3\text{Au}]^+$ (dcpe = 1,2-(dicyclohexylphosphino)ethane), contains two well-separated gold(I) centers, coordinated to three phosphorus atoms in a trigonal planar geometry. It shows emission in both the solid state (501 nm) and in acetonitrile solution (508 nm), with a lifetime for the excited state in solution of 21.1 μs.

The Au(I) complexes of NP_3 show no luminescence in CH_2Cl_2 solution, as would be expected if the coordination remained trigonal. In addition the $^{31}\text{P}\{^1\text{H}\}$ NMR results in CH_2Cl_2 solution suggest that the phosphorus atom coordination is fluxional on a time-scale that is faster than 10⁻⁶ seconds. In our earlier paper on NP_3 complexes [9], we reported that the monomeric gold(I) complex shows a singlet at 26.12 ppm and the binuclear complex $[(\text{NP}_3)_2\text{Au}_2](\text{BPh}_4)_2$ gives two singlets at 25.88 and 27.57 ppm, respectively, in a 2:1 ratio. These spectra were carried out in a $\text{CD}_3\text{CN}/\text{CH}_3\text{CN}$ solution. However, when the $^{31}\text{P}\{^1\text{H}\}$ NMR of the binuclear complex was carried out in a CH_2Cl_2 solution a single

Table 3
Selected interatomic distances (Å) and angles (°) for [(NP₃)Cu](BPh₄), (1)

Cu(1)–N(1)	2.275(7)	P(1)–Cu(1)–P(2)	120.26(10)
Cu(2)–N(2)	2.301(7)	P(1)–Cu(1)–P(3)	121.96(10)
Cu(1)–P(1)	2.264(3)	P(2)–Cu(1)–P(3)	116.56(10)
Cu(1)–P(2)	2.271(3)	P(4)–Cu(2)–P(5)	116.70(11)
Cu(1)–P(3)	2.243(3)	P(4)–Cu(2)–P(6)	119.49(10)
Cu(2)–P(4)	2.265(3)	P(5)–Cu(2)–P(6)	122.33(11)
Cu(2)–P(5)	2.250(3)	P(1)–Cu(1)–N(1)	86.6(2)
Cu(2)–P(6)	2.258(3)	P(2)–Cu(1)–N(1)	85.8(2)
N(1)–C(38)	1.469(11)	P(3)–Cu(1)–N(1)	86.5(2)
N(1)–C(40)	1.493(11)	P(4)–Cu(2)–N(2)	86.5(2)
N(1)–C(42)	1.482(11)	P(5)–Cu(2)–N(2)	85.4(2)
N(2)–C(80)	1.488(12)	P(6)–Cu(2)–N(2)	86.0(2)
N(2)–C(82)	1.491(12)	C(38)–N(1)–C(40)	110.4(7)
N(2)–C(84)	1.478(11)	C(38)–N(1)–C(42)	111.1(7)
Cu(1)⋯P ₃ plane	0.144	C(40)–N(1)–C(42)	110.2(7)
Cu(2)⋯P ₃ plane	0.159	C(80)–N(2)–C(82)	110.7(8)
		C(80)–N(2)–C(84)	110.4(7)
		C(82)–N(2)–C(84)	111.6(8)

peak at 32.49 ppm was obtained and the same peak was found for [(NP₃)₂Au₂](PF₆)₂ in CH₂Cl₂. Cooling this solution does not significantly broaden this peak indicating that the non-equivalent phosphorus atoms are exchanging rapidly in solution. (Exchange may be less rapid in acetonitrile.) Further evidence of this rapid exchange comes from the fact that dissolving the binuclear species in THF causes the complex to be transformed into the mononuclear species. It is well known that gold(I) complexes frequently prefer linear two-coordination, both in the solid state and in solution, and that the three-coordinate species are frequently fluxional. For example, the [(Ph₃P)₃Au]⁺ complex is fluxional in solution, dissociating to [(Ph₃P)₂Au]⁺ and the free ligand. Thus, this observation of this fluxional behavior in the ³¹P{¹H} NMR for the NP₃ complexes is not surprising. The impact of different solvents on the luminescence

of 3-coordinate Au(I) complexes depends on the ease with which equilibria involving 2-coordinate and 3-coordinate complexes are shifted by the solvent. Acidic solvents like CH₂Cl₂ may solvate the non-coordinating phosphine ligands formed upon Au–P bond rupture, stabilizing 2-coordinate species in these solvents while 3-coordinate species form in THF or CH₃CN. Related solvent effects have been reported in water [13].

The Cu(I) complex reported in this paper does not show any visible luminescence, even at 77 K, that can be assigned to metal-centered transitions similar to the ones observed for the 3-coordinate Au(I) complexes. There is a weak emission for the [(NP₃)Cu](BPh₄) complex at low temperatures, but this is assigned to intraligand π,π* transitions, associated with the phenyl rings of the anion [31].

Table 4
Emission maxima and lifetimes of P₃Au complexes in the solid state at 298 K

	λ _{max} (nm) Solid state, 298 K	Lifetime (μs)
[(NP ₃)Au](BPh ₄)	465	1.9, 8.3
[(NP ₃)Au](PF ₆)	494	1.3, 6.3
[(NP ₃)Au]NO ₃	529	0.4, 2.4
[(NP ₃) ₂ Au ₂](BPh ₄) ₂	470	0.7, 7.9
[(NP ₃) ₂ Au ₂](PF ₆) ₂	485	1.3, 5.4

6. Discussion

The structures of the monomeric complexes, [(NP₃)M](PF₆) (M = Au, Ag), both show a trigonally elongated geometry with long M–N distances (Au–N = 2.68 Å, Ag–N = 2.66 Å) and the metals lie out of the plane of the phosphorus atoms, away from the nitrogen (0.41 Å for Au, 0.53 Å for Ag). The Ag(I) nitrate salt, [(NP₃)Ag](NO₃), also has a trigonally elongated structure but the NO₃[−] anion is weakly

coordinated to the silver center in the axial position. The Ag–O distance is 2.55 Å and the Ag atom lies 0.745 Å out of the plane of the phosphorus atoms. In comparison with the Au and Ag complexes, the Cu complex shows more of a trigonal pyramidal geometry. The Cu lies only 0.15 Å out of the P₃ plane. In addition, the Cu–N distances are significantly shorter, 2.275(7) Å and 2.301(7) Å for the two molecules in the asymmetric unit compared with 2.683(6) Å for Au–N and 2.662(3) Å for Ag–N. However, these Cu–N distances are long when compared with previously characterized nitrogen-containing Cu complexes. The Cu–N bond distances are usually in the range 2.04–2.11 Å. This copper–nitrogen interaction, while apparently weak, appears to be stronger than the M–N interactions in the Au(I) and Ag(I) analogs. The M–N bond distance trend is Cu > Ag ~ Au.

Of the three monomeric complexes, [(NP₃)M]⁺ (M = Au, Ag, Cu), only the gold complexes show a strong luminescence at 77 K. In addition, the gold binuclear species, [(NP₃)₂Au₂](BPh₄)₂ also shows strong emissions at low temperatures. In this latter complex, two of the phosphorus atoms of each ligand chelate to one gold atom while the third phosphorus atom bridges to the other gold atom. Thus, each gold is three-coordinate and approximately trigonal planar, with no interaction between the gold and nitrogen centers. The large Stokes' shifts between the excitation and emission energies, shown in Table 4, for the gold complexes, imply that the emission is phosphorescence and the long lifetimes measured (>2 μs) confirm this assignment. The values of the emission maxima are all in the range 465–529 nm, indicating that the origin of the emission is likely to be the same for all the complexes measured. This emission has been assigned as an essentially metal-centered triplet to singlet transition $a_2''(p_z) \rightarrow e'(d_{x^2-y^2}, d_{xy})$. This assignment is the same as that made for related P₃Au trigonal planar systems and the platinum(0) complexes [32]. The [(NP₃)Au]⁺ complexes show shifts in the emission energies, depending on the anion used. However, none of the anions interact directly with the gold(I) centers and there is no obvious correlation between the anion used and the emission energy. The small differences in emission energy maxima are thought to be due to conformation differences in the molecules and packing effects.

In solution, the ³¹P{¹H} NMR results indicate that the phosphorus groups are fluxional. The observation of this fluxional behavior may explain the absence of emission in solution, where the three-coordinate P₃Au unit does not exist in solution long enough for emission from the triplet excited state to occur.

The failure of the [(NP₃)Cu]BPh₄ complex to show a visible luminescence, as found for the [(NP₃)Au]⁺, is probably attributable to the fact that the Cu(I) is not 3-coordinate, although this seemed like a reasonable possibility from the Au(I) and Ag(I) work. The luminescence found in 3-coordinate phosphine complexes of Au(I) is quenched when the Au(I) becomes 4-coordinate. The fact that the NP₃ ligand product is four coordinates in Cu(I) and only three coordinate with Au(I) and Ag(I) must be attributed to the smaller size of Cu(I) and its increased tendency for full sp³ orbital hybridization, compared especially with Au(I), where relativistic effects impact on the orbital mixing. With Ag(I), the data are not clear as to why the Ag...N distance is long, 2.662 Å. Consequently the question of the possible existence of visible luminescence in 3-coordinate Cu(I) complexes with phosphine ligands remains open.

Supplementary material available for complex **1**, including tables of crystallographic data, atomic coordinates, thermal parameters and bond distances and angles (18 pages) is available. Ordering information is given on any current masthead page. Tables of structure factors (76 pages) are available from John P. Fackler, Jr upon request.

Acknowledgements

Luminescence lifetime measurements were obtained at the Center for Fast Kinetics Research, which is jointly supported by the Biotechnology Branch of Research Sources of the NIH (Grant RR00886) and by The University of Texas at Austin. This work was supported by the National Science Foundation (Grant CHE 9300107) and the Welch Foundation.

References

- [1] C. Mealli, C.A. Ghilardi, A. Orlandini, *Coord. Chem. Rev.* 120 (1992) 361.

- [2] C. Bianchini, D. Masi, C. Mealli, A. Meil, M. Sabat, G. Scapacci, *J. Organomet. Chem.* 273 (1984) 91.
- [3] L. Sacconi, A. Orlandini, S. Midollini, *Inorg. Chem.* 13 (1974) 2850.
- [4] F. Cecconi, C.A. Ghilardi, S. Midollini, S. Moneti, A. Orlandini, G. Scapacci, *J. Chem. Soc. Dalton Trans.* (1989) 211.
- [5] C.A. Ghilardi, S. Midollini, S. Moneti, A. Orlandini, *J. Chem. Soc. Chem. Commun.* (1986) 1771.
- [6] L. Sacconi, C.A. Ghilardi, C. Mealli, F. Zanobini, *Inorg. Chem.* 14 (1975) 1380.
- [7] C. Mealli, L. Sacconi, *J. Chem. Soc. Chem. Commun.* (1973) 886.
- [8] M.N.I. Khan, R.J. Staples, C. King, J.P. Fackler Jr., R.E.P. Winpenny, *Inorg. Chem.* 32 (1993) 5800.
- [9] U.M. Tripathi, A. Bauer, H. Schmidbaur, *J. Chem. Soc. Dalton Trans.* (1997) 2865.
- [10] T.M. McCleskey, H.B. Gray, *Inorg. Chem.* 31 (1992) 1734.
- [11] C. King, M.N.I. Khan, R.J. Staples, J.P. Fackler Jr., *Inorg. Chem.* 31 (1992) 3236.
- [12] J.M. Forward, R.J. Staples, C.W. Liu, J.P. Fackler Jr., *Acta Cryst. C* 53 (1997) 195–197.
- [13] J.M. Forward, Z. Assefa, J.P. Fackler Jr., *J. Am. Chem. Soc.* 117 (1995) 9103.
- [14] J.M. Forward, J.P. Fackler Jr., Z. Assefa, in: M. Roundhill, J.P. Fackler Jr. (Eds.), *Optoelectronic Properties of Inorganic Compounds*, Plenum, New York, 1997, 195–229.
- [15] P.D. Harvey, H.B. Gray, *J. Am. Chem. Soc.* 110 (1988) 2145.
- [16] P. Leoni, G. Chiaradonna, M. Pasquali, F. Marchetti, A. Fortunelli, G. Germano, *Inorg. Chimica Acta* 264 (1997) 185.
- [17] C.E. Moore, *Atomic Energy Levels*, U.S. Department of Commerce, NBS circular 467 (1958).
- [18] J.P. Fackler Jr., Z. Assefa, J.M. Forward, R.J. Staples, *Metal Based Drugs* 1 (1994) 469.
- [19] L. Sacconi, I. Bertini, *J. Am. Chem. Soc.* 90 (1968) 5443.
- [20] CAChe, *Computer Aided Chemistry*, CAChe Scientific Inc., Beaverton, Oregon, 1994.
- [21] N.L. Allinger, *J. Am. Chem. Soc.* 99 (1977) 8127.
- [22] W.R. Scheidt, I. Turowska-Tyrk, *Inorg. Chem.* 33 (1994) 1314.
- [23] J. Pflugrath, A. Messerschmitt, MADNES, Munich Area Detector (New EEC) System, version EEC 11/9/89, with enhancements by Enraf–Nonius Corp., Delft, The Netherlands. A description of MADNES appears in; A. Messerschmitt, J. Pflugrath, *J. Appl. Crystallogr.* 20 (1987) 306.
- [24] M.S. Lehman, F.K. Larsen, *Acta Crystallogr.* A30 (1974) 580.
- [25] C. Wilkinson, H.W. Khamis, in: P. Convert, J.B. Foryth (Eds.) *Position Sensitive Detection of Thermal Neutrons*, Academic Press, New York, 1983; p 358.
- [26] R.F.D. Stansfield, G.J. McIntyre, *Neutron Scattering in the Nineties*, IAEA, Vienna, 1985, p 191.
- [27] W.J. Kabsch, *J. Appl. Cryst.* 21 (1988) 67.
- [28] W. Kabsch, *J. Appl. Cryst.* 21 (1988) 916.
- [29] G.M. Sheldrick, *SHELXL-93 Program for Crystal Structure Refinement*, University of Göttingen, Germany, 1993.
- [30] T.M. McCleskey, J.R. Winkler, H.B. Gray, *Inorg. Chim. Acta* 225 (1994) 319.
- [31] D.P. Segers, M.K. DeArmond, P.A. Grutsch, C. Kotal, *Inorg. Chem.* 23 (1984) 2874.
- [32] D.M. Roundhill, *Photochemistry and photophysics of metal complexes*. Plenum Press, N.Y., 1994, 84–88.